European Journal of Pharmaceutics and Biopharmaceutics 199 (2024) 114308

Contents lists available at ScienceDirect

European Journal of Pharmaceutics and Biopharmaceutics

journal homepage: www.elsevier.com/locate/ejpb

Hydrogel formats to model potential drug interactions occurring at the subcutaneous injection site

Conor Gomes [a], Kate Gridley [b], Imogen Anastasiou [a], Bálint Sinkó [a], Randall J. Mrsny [b,*]

[a] Pion, Inc., Billerica, MA 01821, USA
[b] Department of Life Sciences, Centre for Therapeutic Innovation, University of Bath, Bath BA2 7AY, UK

ARTICLE INFO

Keywords:
Subcutaneous injection
Extracellular matrix
In vitro model
Drug fate

ABSTRACT

We have previously developed an *in vitro* instrument, termed subcutaneous injection site simulator (SCISSOR), that can be used to monitor release properties of an active pharmaceutical ingredient (API) and formulation components of a medicine designed for SC injection. Initial studies to validate the SCISSOR instrument applications used a simple hyaluronic acid (HA) hydrogel to monitor early release events. We now report a type of cross-linked HA that can, when combined with HA, provide a hydrogel (HA-XR) with optical clarity and rheological properties that remain stable for at least 6 days. Incorporation of 0.05–0.1 mg/mL of collagens isolated from human fibroblasts (Col F), bovine type I collagen (Col I), chicken collagen type II (Col II), or chondroitin sulphate (CS) produced HA or HA-XR hydrogel formats with optical clarity and rheological properties comparable to HA or HA-XR alone. HA + Col F hydrogel had a much greater effect on release rates of 70 kDa compared to 4 kDa dextran, while Col F incorporated into the HA-XR hydrogel accentuated differences in release rates of prandial and basal forms of insulin as well as decreased the release rate of denosumab. A hydrogel format of HA + Col I was used to examine the complex events for bevacizumab release under conditions where a target ligand (vascular endothelial growth factor) can interact with extracellular matrix (ECM). Together, these data have demonstrated the feasibility of using a cross-linked HA format to examine API release over multiple days and incorporation of specific ECM elements to prepare more biomimetic hydrogels that allow for tractable examination of their potential impact of API release.

1. Introduction

Subcutaneous (SC) injection is commonly used to deliver drugs that are inadequately or inconsistently absorbed following oral administration, most notable among these are protein and peptide therapeutics as well as nucleic acid-based materials. Despite the common use of SC injections, such administrations rarely reach 100 % bioavailability for an active pharmaceutical ingredient (API). While a number of factors could be at play, specific events that could affect API release from a SC injection site are still poorly understood [1]. Some SC injection site events that could reduce the extent of biologically active API reaching the systemic circulation include API degradation as well as interaction(s) between the API and extracellular matrix (ECM) elements, potentially leading to extensive binding and/or precipitation.

Pharmaceutical companies use thousands of animals every year to test candidate formulations intended for SC injection. The value of such studies, however, must be questioned as no pre-clinical animal model has yet been identified to predict the performance of these SC formulations in humans. These discrepancies may reflect differences between the organization and composition of human hypodermis and the various eutherian species used as preclinical models for assessing formulations intended for SC injection [2]. While such animal studies are needed to assess safety prior to clinical testing, lack of a predictable clinical results limit the identification of a formulation with the desired behavior for a safe and efficacious outcome. Initial testing of a drug formulation in humans based upon data obtained from a non-predictive animal model could be misleading. In the case where a formulation results in an unexpected lack of exposure, a promising drug might be shelved as there is no model to understand why that formulation failed and how to select one that might succeed. Worse yet, a formulation with an inaccurately

Abbreviations: HA, Hyaluronic acid; CL-HA, Crosslinked HA; HA-XR, Mixture of CL-HA and HA; Col I, Bovine type I collagen; Col II, Chicken type II collagen; Col F, Collagens isolated from human fibroblast culture; CS, Chondroitin sulfate; SCISSOR, Subcutaneous Injection Site Simulator; PBS, Phosphate buffer saline.

* Corresponding author at: University of Bath, Department of Life Sciences and Centre for Innovative Therapeutics, Claverton Down, Bath BA2 7AY, UK.
E-mail address: Rjm37@bath.ac.uk (R.J. Mrsny).

https://doi.org/10.1016/j.ejpb.2024.114308
Received 30 January 2024; Received in revised form 13 April 2024; Accepted 28 April 2024
Available online 28 April 2024

predicted marginal uptake following SC injection could lead to dangerous overexposure outcomes when tested in humans.

In the case of biopharmaceuticals, such as protein and peptide therapeutics, these drugs are often formulated at a non-physiologic pH and commonly with a variety of stabilizing agents that include combinations of sugars, salts, and surfactants. Following SC injection, these low molecular weight formulation components may leave the injection site more rapidly than a high molecular weight biopharmaceutical as the hypodermis reestablishes its homeostatic conditions. During this transition, biopharmaceuticals may transition thought their isoelectric point of lowest solubility, putting them at risk of precipitation. The ECM is composed of a variety of proteins such as collagen and elastin, as well as glycosaminoglycans such as hyaluronic acid (HA) and chondroitin sulfate (CS) [3]. Some APIs may bind tightly with ECM elements, for example some growth factors can bind to collagen [4] and some proteins can have specific interactions with various proteoglycans [5]. It is possible that such events could affect API release from the SC injection site, supporting the premise that an *in vitro* tool which included some of these elements could be used to examine potential precipitation and binding events between a formulation and ECM components. Such a tool could provide a tractable method to guide pharmaceutical scientists during formulation screening. To this end, an analytical instrument, termed SCISSOR (subcutaneous injection site simulator) was developed and is currently marketed by Pion, Inc.

The SCISSOR instrument uses a 'cartridge' composed of a cuvette enclosed on two sides with dialysis membrane and containing an optically clear artificial extracellular matrix (aECM) used to model the injection site. The cartridge is positioned in a chamber containing physiologically relevant buffer meant to mimic interstitial fluid (ISF) of the hypodermis and provides a means to emulate the infinite sink of the body. This artificial ISF is a complex bicarbonate buffer-based mixture designed to replicate physiological aspects comparable to human blood, maintained at a pH of ~ 7.4, within a narrow osmotic range and at a temperature of ~ 34 °C [6]. By simultaneously monitoring the solubility of a formulation injected into an aECM and correlating this outcome with measurement of an API within the simulated ISF over time, a pharmaceutical scientist can examine parameters of formulation performance without the use of animals. While such SCISSOR studies are not intended to completely recreate the three-dimensional network present in the human hypodermis, introduction of specific ECM elements within the cartridge can be used to model the impact of specific hypodermis elements in a tractable manner and address hypothesis-driven questions concerning formulation development.

We initially set up the SCISSOR instrument with injection site cartridges containing HA and examined its performance by comparing outcomes with clinical, not preclinical, formulation performance using human pharmacokinetic and bioavailability information for eight monoclonal antibodies (mAbs) [7]. Compared with data obtained from preclinical monkey and mini pig studies, the SCISSOR provided more accurate prediction for clinical outcomes for all eight mAbs. Having validated the clinical value of the SCISSOR with an injection cartridge format containing HA for formulations intended to have the API leave the SC injection site within hours, we now examine the feasibility of hydrogels for extended-release formulations and the impact of specific ECM elements. Herein, we describe a novel crosslinked format of HA (HA-XR) that is more amenable than the previous HA-containing model for monitoring drug release over extended periods of time, as well as hydrogels where a complex of collagens from human fibroblasts (Col F), bovine type 1 collagen (Col I), chicken type 2 collagen (Col II), or chondroitin sulphate (CS) have been introduced. Our data identify parameters where ECM components could be integrated into HA or HA-XR formats in a way that has minimal impact on the optical clarity and rheological properties of these hydrogels. By having these similar properties, assessment of API solubility and drug release profile differences can be made to directly reflect the impact of an ECM element on API stability and release that is not merely due to changes in optical and viscoelastic characteristics. This expanded repertoire of hydrogel matrices should provide additional tools to model potential interactions that could occur at the SC injection site, informing drug candidate selection and/or SC injection formulation design.

2. Materials and methods

2.1. Preparation of hydrogels for early- (HA) and extended-release (HA-XR) formats

Pion Inc. has developed methodologies to produce aECMs for use within the SCISSOR platform. Briefly, hydrogels were prepared by adding hyaluronic acid from *Streptococcus equi* (Sigma, 53747) to a beaker of phosphate buffer solution and stirred overnight to achieve a concentration of 6.25 mg/mL. Col F (Sigma, C2249), Col I (Sigma, C2124), Col II (Sigma, C9301), or CS (Sigma, C6737) was added to HA solutions in the last 2 min of stirring to achieve a desired final concentration. Hydrogels were then placed in a VacMaster VP215 vacuum chamber for 2 x 1 min cycles. After degassing the solution, it was aspirated into 5 mL syringes and stored at 10 °C until use. For each iteration of component concentration, the optical clarity was assessed by visual inspection in 1 cm path-length PMMA semi-micro spectrophotometry cuvettes (VWR) and absorbance was measured at 600 nm using a NanoDrop 2000 (Thermo Scientific). Samples were initially stored at 4 °C for 24 h and subsequently incubated at 34 °C for 24 h. HA-XR gels were supplied by Pion Inc., USA as part of the ECM-XR cartridge packs purchased. The HA-XR (also known as ECM-XR) comprises a stabilized crosslinked HA-based hydrogel, which was designed to exhibit a slower material release from the SCISSOR cartridge compared to HA. Other matrices mentioned in this paper (Col F, Col I, Col II, and CS) were added to these HA and HA-XR formats to provide systemics with additional elements in the hypodermis that could affect the performance of an injected formulation. These were prepared by inclusion of Col F, Col I, Col II, or CS and, in the case of HA-XR, were followed by degassing for 1–2 min prior to cross-linking of the HA.

2.2. Rheological analysis

Samples were analyzed using an Anton Paar MCR102e rheometer with a 50 mm sandblasted plate-plate geometry. Hydrogel platforms are typically analyzed using an oscillating frequency and low strain values shown to limit the potential for sample destruction for similar hydrogel matrices of this type [8]. For unadulterated samples, a 2.5 mL solution was loaded onto the stage by expressing the material from a 5 mL syringe at 2.5 cm/min. 7.0 mL of deionized water was pipetted around the stage to maintain a hydrated environment. The sample was analyzed at an oscillating frequency from 0.1-100 rad/s @ 1 % strain and 28 °C. This temperature was selected to inhibit evaporation as much as possible while eliminating the effects of ambient temperature during analysis. For samples analyzed after a SCISSOR assay, with the entirety of cartridge contents being poured from the cuvette onto the rheometer stage. The entire 5 mL of sample of each hydrogel to be tested was poured form the cuvette onto a 25 mm plate-plate geometry stage, with contents being kept hydrated by surrounding the stage with 3–4 mL of deionized water. Samples were then analyzed at an oscillating frequency from 0.1-100 rad/s @ 1 % strain and 28 °C.

2.3. Test molecules examined

Texas Red®-labeled dextran of average 4,000 (FD4) or 70,000 (FD70) molecular weights, and caffeine were purchased from Sigma. Bevacizumab and vascular endothelial growth factor ($VEGF_{165}$) were kindly provided by Genentech through their reagent procurement program. The monoclonal antibody denosumab (Prolia®), as well as fast-acting (prandial) Actrapid® and slow-acting (basal) Levemir® insulins were sourced from a local pharmacy.

Table 1
Parameters of test materials and analytics used for the studies described.

Test Material	Method of Analysis
Caffeine	Direct peak @ 272 nm
Insulin Rapid	2nd derivative peak @ 286 nm
Insulin Basal	Integrate 2nd derivative peak from 264-280 nm
Dextran-FITC-CM (4 kDa)	Direct peak @ 496
Dextran Texas Red® (70 kDa)	2nd derivative peak @ 594 nm
Denosumab	2nd derivative peak @ 300 nm

2.4. Test molecule release protocol

The SCISSOR instrument was obtained from Pion, Forest Row, UK. Each injection and analysis methodology has multiple publications and case studies validating their application and performance with the Pion Resource Library [9]. Prior to testing the release of a molecule, each aECM-containing cassette was allowed to equilibrate to 34 °C in the SCISSOR instrument for 30 min in a bicarbonate-based buffer that mimicked interstitial fluid (ISF) and provided "infinite sink" conditions. ISF contained 6.4 g NaCl, 0.09 g $MgCl_2{\cdot}6H_2O$, 0.4 g KCl, 0.2 g $CaCl_2$, 0.2 g NaN_3, and 2.1 g $NaHCO_3$ in dissolved in 1 L Milli-Q water and maintained by the SCISSOR instrument at 34 °C and pH 7.4 by flowing CO_2(g) on top of the solution. For all injectates, a 200 μL aliquot was introduced into the cartridge via an Eppendorf Repeater® E3 pipette fitted with a 1 mL Eppendorf Combitip advanced pipette tip through a 25G x 5/8"Med Vet International Terumo needle at a rate of 15 μL/s. Optical clarity of hydrogels was monitored using the onboard LEDs and cameras of the SCISSOR. API release was monitored via in situ fiber-optic UV–Vis probes using the Rainbow spectrophotometer unit (Pion Inc., USA). All formulations were analyzed in triplicate, unless otherwise stated.

2.5. Data analysis

Release curves were analyzed in situ using Pion's AuPro software, as well as offline analysis with an Agilent A1100 HPLC after sampling. All error bars indicate standard deviation, and statistical significance was given by a $p < 0.05$ with Student's *t*-test (n = 3, unless stated otherwise). A table describing each spectrophotometric method used to measure API release is shown below (Table 1).

For the detection of bevacizumab, a reversed phase high performance liquid chromatography method was used [10], with some modifications. Specifically, aliquots taken from the infinite sink chamber were analyzed by high performance liquid chromatography using an Agilent 1100 HPLC system fitted with a Zorbax 300SB-C8 Narrow-bore column with 5 μm particle size, 300 Å wide-pore, 2.1 mm internal diameter and 150 mm length from Agilent Technologies (Santa Clara, CA, U.S.A.). Chromatographic analysis was performed at a flow rate of 1.0 mL/min in a gradient mode with eluents comprising 0.1 % TFA in ultra-pure water (eluent A) and 0.1 % TFA in acetonitrile (eluent B). The gradient started at 10 % of eluent B, increasing to 45 % of B in 4 min, and kept constant at 45 % of B for 3 min. From 7–7.1 min, eluent B decreased to 30 %, and was kept constant until 10 min. From 10-10.1 min eluent B was decreased to 0 % until 14.4 min, after which it was raised to 10 % by 14.5 min and was maintained at 10 % until 15 min. The injection volume was 30 μL and the column oven was maintained at 75 °C.

3. Results

3.1. Hydrogel optical and rheological properties

Previous studies using the SCISSOR instrument used cartridges filled with HA, providing an optically clear matrix for studies occurring over a time course of only a few hours [6,7]. A significant amount of HA, however, can release from the cartridge through the dialysis membrane over extended periods of time (days), limiting applications of this HA format for extended-release studies to assess long-acting injectable (LAI) formulations. Indeed, after 72 h (T_{72}) of incubation of 6.25 mg/mL HA in ISF maintained at 34 °C and pH 7.4, the hydrogel matrix lost almost all its viscoelastic properties, approaching complex viscosities comparable to water (10^{-3} Pa·s) (Fig. 1**A**). Introduction of a collagen mixture secreted from human fibroblasts (Col F) at 0.05 mg/mL into 6.25 mg/mL HA resulted in a hydrogel with viscosities, measured at 0.2–100 rad/s and 1 % strain, that were statistically similar ($p > 0.05$) to 6.25 mg/mL HA at T_0 (Fig. 1**A**). Rheometric analysis at 1 % strain was chosen as it lies near the midpoint of the linear viscoelastic region of these hydrogels (data not shown). When rheometric properties were measured at T_{72}, the HA + Col F hydrogel format retained significantly more viscosity ($p < 0.05$) over the sweep range of 2–60 rad/s compared to the HA

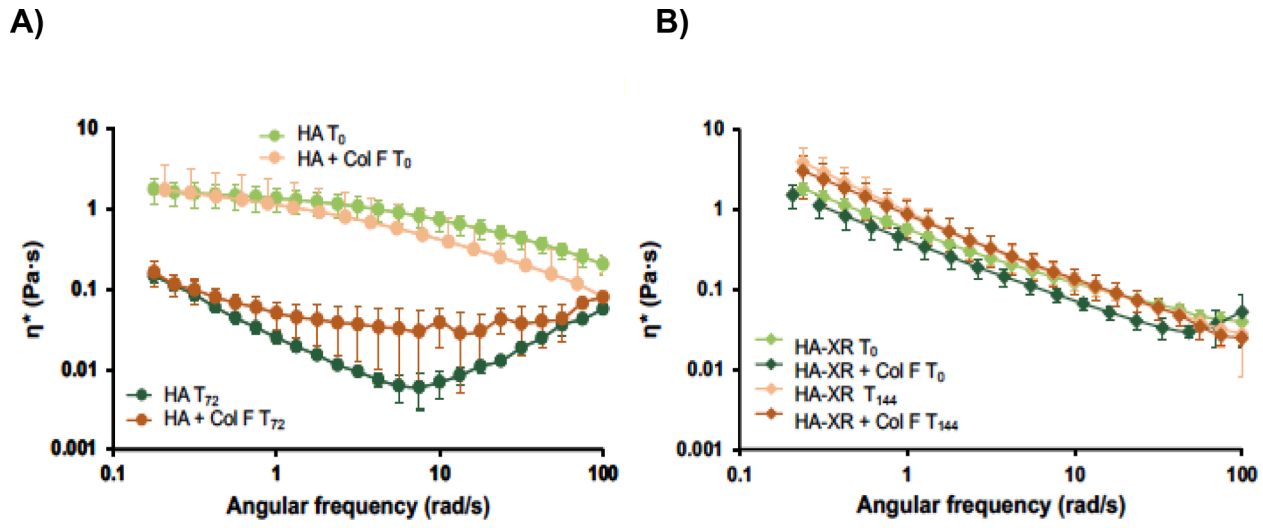

Fig. 1. Impact of collagen and/or crosslinking on hyaluronic acid (HA) hydrogels. (**A**) Complex viscosity measured from 0.2-100 rad/s @ 1 % strain for angular frequency scans defining rheological properties of 6.25 mg/mL HA (light orange) or 6.25 mg/mL HA combined with 0.05 mg/mL Col F (light green) at the time of preparation and these same mixtures shown in dark orange and dark green, respectively, after 72 h (T_{72}) of incubation in the SCISSOR system bicarbonate-based buffer to emulate interstitial fluid at the subcutaneous injection site (n = 3). (**B**) Similar angular frequency scans of 0.8 mg/mL cross-linked HA (CL-HA) mixed with 2.0 mg/mL HA (HA-XR) and combined with 0.05 mg/mL Col F at the time of preparation and these same mixtures shown in dark orange and dark green, respectively, after 144 h of incubation (T_{144}) in the SCISSOR system (n = 3). Error bars = standard deviation of repeated runs. Complex viscosity (η*, Pa·s ± SD), shown as a function of angular frequency, was measured from 0.2-100 rad/s at 1 % strain in all cases.

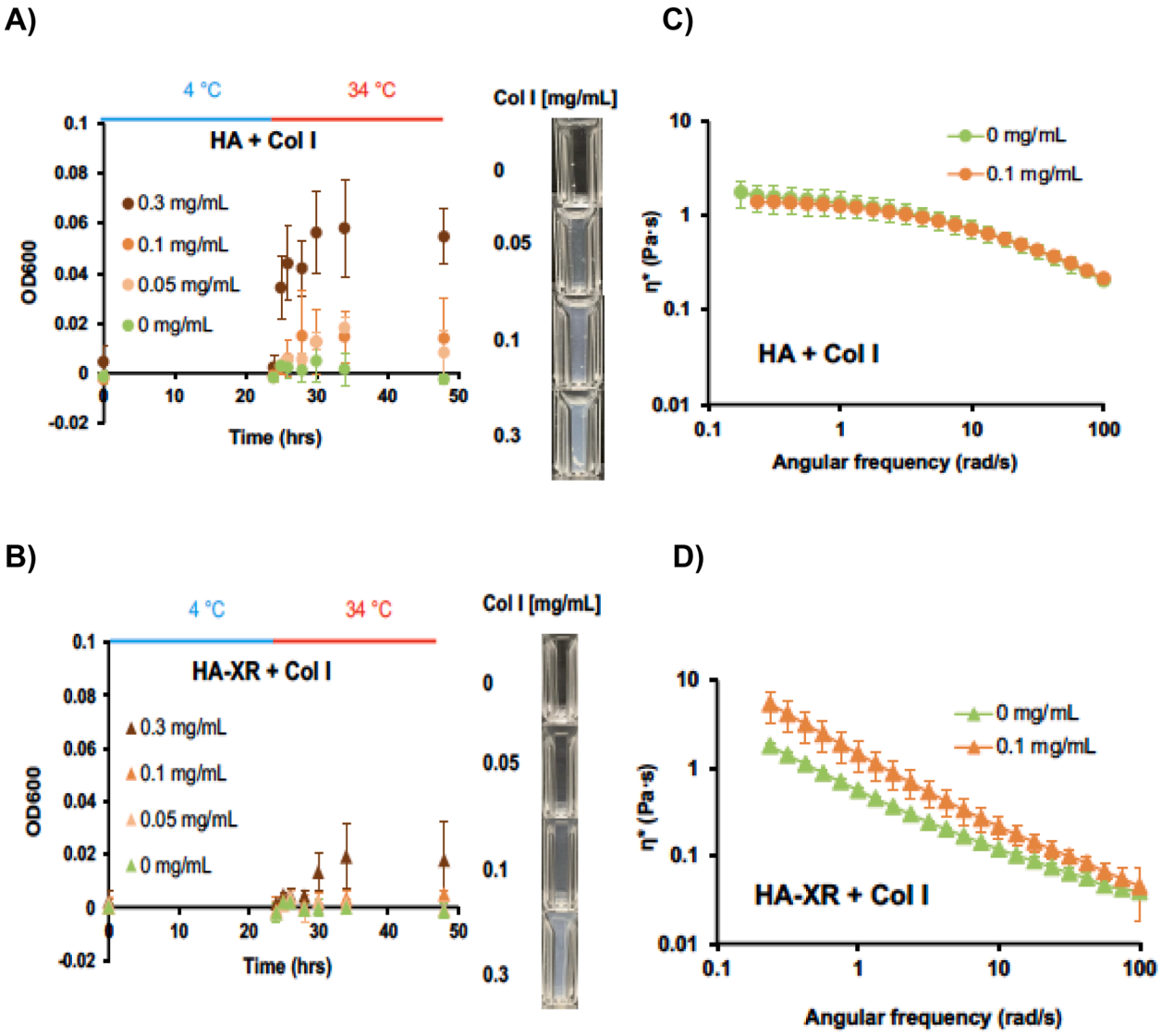

Fig. 2. Impact of bovine type I collagen (Col I) at 0.05, 0.1, or 0.3 mg/mL integrated into 6.25 mg/mL hyaluronic acid (HA) or 0.8 mg/mL cross-linked HA + 2.0 mg/mL HA (HA-XR) hydrogels. Assessment of optical clarity of (**A**) HA and (**B**) HA-XR hydrogels containing varying amounts of Col I, where OD_{600} data represents n = 3 ± SEM with example cuvettes to enable a visual appreciation of relative opacity. Angular frequency scans defining rheological properties of (**C**) HA with and without 0.1 mg/mL added Col I or (**D**) HA-XR hydrogels with and without 0.1 mg/mL added Col I. Complex viscosity (η *, Pa·s ± SD), shown as a function of angular frequency, was measured from 0.2-100 rad/s at 1 % strain in all cases.

hydrogel (Fig. 1**A**).

As the lag time of spontaneous collagen assembly is slowed by the presence of negatively charged glycosaminoglycans [11], we assumed that Col F introduced into the negatively changed HA hydrogel acted to essentially non-covalently cross-link this matrix to slow its loss from the SCISSOR cartridge. If so, we would predict that a stabilized matrix within the cartridge could provide a hydrogel more appropriate for extended-release studies. To further test the concept of increased matrix interactions, a cross-linked version of HA (CL-HA) was developed. Combining 0.8 mg/mL CL-HA with 2.0 mg/mL HA (HA-XR) produced a hydrogel that retained viscoelastic properties after 144 h (T_{144}) in the SCISSOR system; incorporation of 0.05 mg/mL Col F into HA-XR showed viscosities at T_0 and T_{144} similar to HA-XR ($p > 0.05$) over the 0.2–100 rad/s range (Fig. 1**B**). Importantly, the rheological properties of the HA-XR matrix were not affected by incorporation of Col F, supporting the suitability this-XR format for testing LAI formulations.

We next examined the impact of including ECM elements, including bovine type I collagen (Col I), chicken type II collagen (Col II), a mixture of collagens secreted by human fibroblasts (Col F), and chondroitin sulfate (CS), on HA-based hydrogel properties to identify ratios of ECM components that could be used to examine the impact of these elements on API release. The goal was to identify ratios that retained sufficient optical clarity to allow for real-time drug solubility/stability analysis and rheological properties comparable to HA or HA-XR hydrogels alone to enable direct assessment of these additional ECM elements on the fate of injected APIs.

Systems containing a final concentration of 0.05, 0.1, or 0.3 mg/mL Col I were prepared by stirred mixing at 4 °C of 6.25 mg/mL HA or 0.8 mg/mL CL-HA with 2.0 mg/mL HA (HA-XR) with the appropriate amount of Col I. After preparation, samples were stored at 4 °C for 24 h to mimic conditions of production and storage/shipping before being warmed to 34 °C for 24 h in an incubator to reflect experimental use. Optical density of these hydrogel formats measured over this time course at 600 $_{nm}$ demonstrated that all HA/Col I formats tested were optically clear at 4 °C. Upon warming to 34 °C, there was an appreciable increase in opaqueness that was directly correlated with the level of Col I (Fig. 2**A**). A similar set of Col I-containing hydrogels were prepared in HA-XR. Like the HA-based materials, these HA-XR/Col I hydrogels were

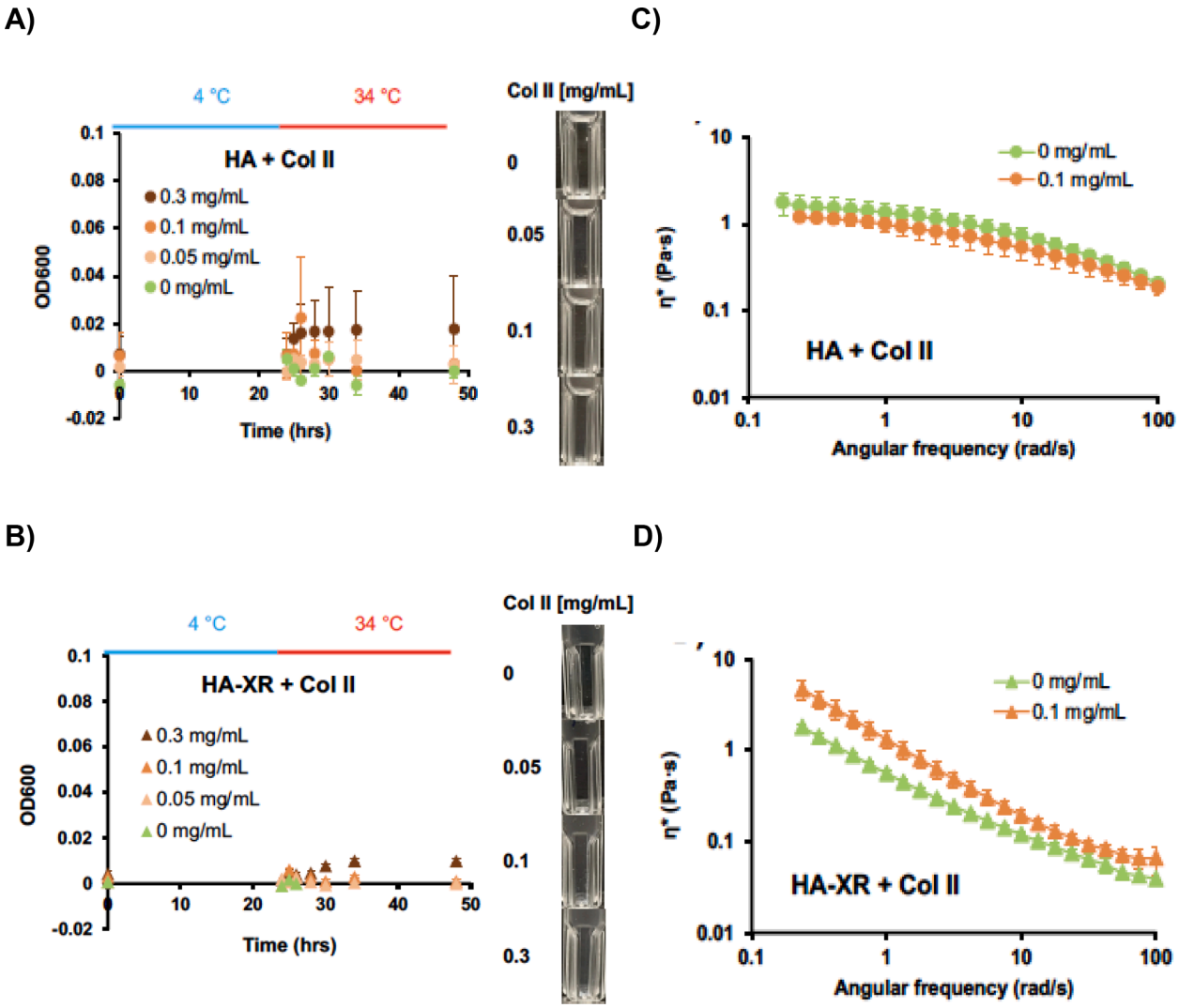

Fig. 3. Impact of chicken type II collagen (Col II) at 0.05, 0.1, or 0.3 mg/mL integrated into 6.25 mg/mL hyaluronic acid (HA) or 0.8 mg/mL cross-linked HA + 2.0 mg/mL HA (HA-XR) hydrogels. Assessment of optical clarity of (**A**) HA and (**B**) HA-XR hydrogels containing varying amounts of Col II, where OD_{600} data represents n = 3 ± SEM with example cuvettes to enable a visual appreciation of relative opacity. Angular frequency scans defining rheological properties of (**C**) HA with and without 0.1 mg/mL added Col II or (**D**) HA-XR hydrogels with and without 0.1 mg/mL added Col II. Complex viscosity (η*, Pa·s ± SD), shown as a function of angular frequency, was measured from 0.2-100 rad/s at 1 % strain in HA and HA-XR formats.

optically clear at 4 °C but acquired opacity upon warming to 34 °C, the extent of which was positively correlated with increasing Col I (Fig. 2**B**). Notably, the Col I-dependent increase in opacity was greater in HA hydrogels (Fig. 2**A**) than that observed for HA-XR hydrogels (Fig. 2**B**). HA + 0.1 mg/mL Col I demonstrated similar rheological properties as HA sans collagen (Fig. 2**C**). HA-XR + 0.1 mg/mL Col showed increasing yield stress at lower angular frequencies compared to HA-XR, consistent with additional entanglement events that might be expected by combining a protein with amphipathic peptide sequence motifs of collagen capable of forming quaternary structures to increase points of hydrogel interaction and add to rheological complexity (Fig. 2**D**).

A similar study was performed with chicken type II collagen (Col II). Like the outcomes observed for Col I, Col II-containing hydrogels prepared at 4 °C were optically clear and the level of acquired opacity upon warming to 34 °C was directly related to the level of Col II for both 6.25 mg/mL HA (Fig. 3**A**) and 2.0 mg/mL HA with 0.8 mg/mL CL-HA (HA-XR) formats (Fig. 3**B**), with the latter again showing less opacity for the same level of Col II content. Notably, the prominent collagen present in the vitreous humor of the eye is type II [12], consistent with its substantially greater transparency in these HA and HA-XR hydrogels compared to Col I-containing matrices. Hydrogels containing 0.1 mg/mL Col II prepared with HA demonstrated rheological properties comparable to those of HA alone (Fig. 3**C**). Like our observations with Col I (Fig. 2**D**), the increased viscosity of HA-XR + 0.1 mg/mL Col II versus HA-XR were consistent with the higher shear rate needed to induce flow due to increased crosslinking complexity (Fig. 3**D**). Thus, bovine type I and chicken type II collagens can be integrated into HA and HA-XR hydrogel formats and appear to be of sufficient optical clarity and limited rheological impact to allow assessment of potential API interactions using the *in vitro* SCISSOR model format.

While hydrogels containing these non-human collagen sources could be used to assess certain collagen-specific interactions involving an API, we also examined a mixture of collagens secreted by human fibroblasts (Col F), which is predominantly composed of amphipathic type I collagen [13], as a format to provide a more clinically relevant hydrogels to assess SC injected formations. Col F-containing hydrogels prepared at 4 °C were optically clear and the level of acquired opacity upon warming to 34 °C was directly related to the level of Col F for both HA (Fig. 4**A**) and HA-XR (Fig. 4**B**). Inclusion of Col F into HA resulted in hydrogels with optical clarity more comparable to Col I (Fig. 2) than Col II (Fig. 3) hydrogels. HA hydrogels prepared with added 0.1 mg/mL Col F demonstrated complex rheological properties comparable to HA alone

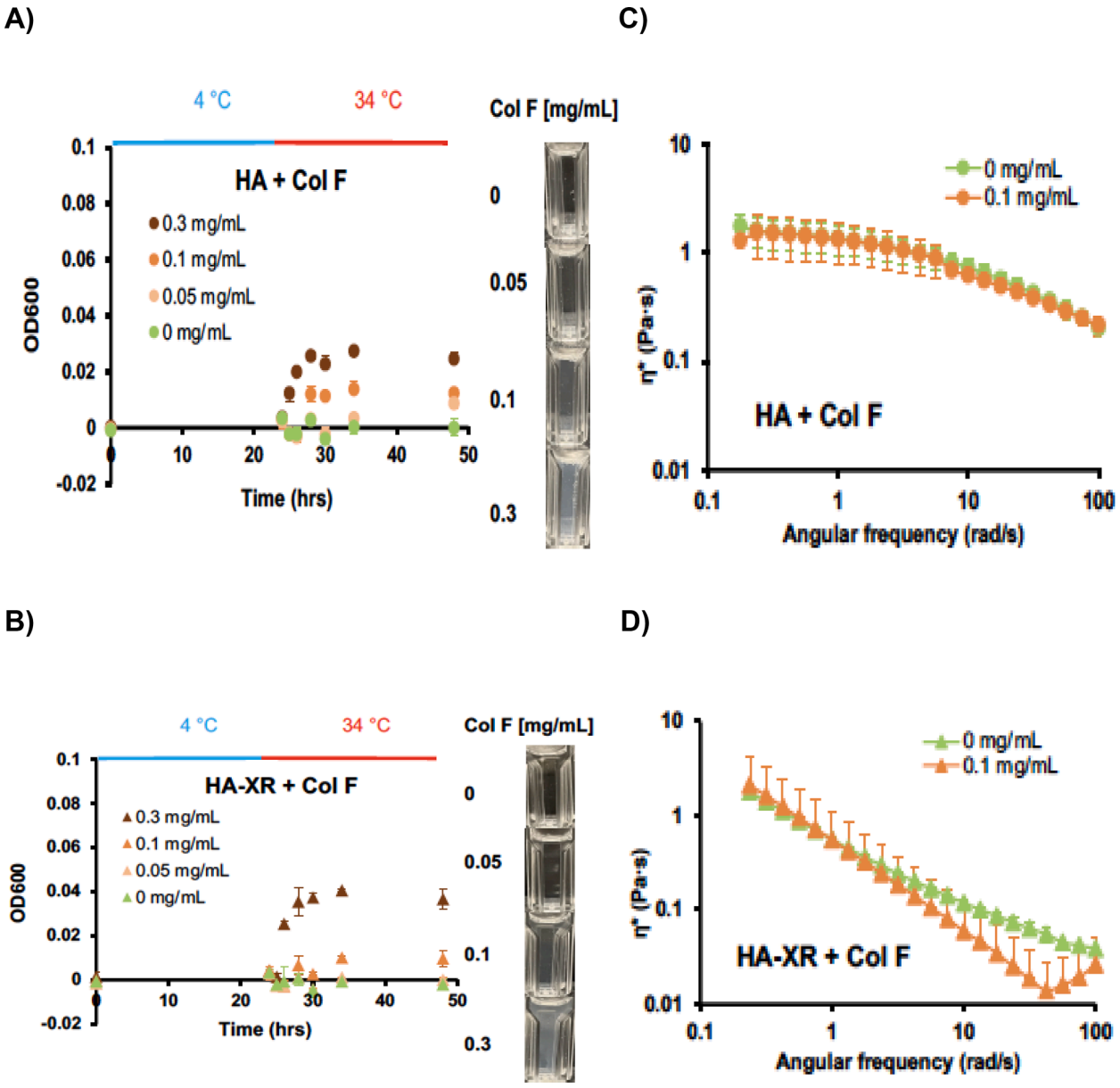

Fig. 4. Impact of collagens isolated from human fibroblasts (Col F) at 0.05, 0.1, or 0.3 mg/mL integrated into 6.25 mg/mL hyaluronic acid (HA) or 0.8 mg/mL cross-linked HA + 2.0 mg/mL HA (HA-XR) hydrogels. Assessment of optical clarity of (**A**) HA and (**B**) HA-XR hydrogels containing varying amounts of Col F, where OD_{600} data represents n = 3 ± SEM with example cuvettes to enable a visual appreciation of relative opacity. Angular frequency scans defining rheological properties of (**C**) HA or (**D**) HA-XR hydrogels with and without 0.1 mg/mL added Col F. Complex viscosity (η*, Pa·s ± SD), shown as a function of angular frequency, was measured from 0.2-100 rad/s at 1 % strain in HA and HA-XR formats.

(Fig. 4**C**). HA-XR and HA-XR + 0.1 mg/mL Col F hydrogels showed comparable rheological properties at low angular frequencies but differed at higher frequencies (Fig. 4**D**). Notably, the complex viscosity of the HA-XR + Col F decreased with increase angular frequency until ~ 50 rads/sec was reached when further increasing the angular velocity resulted in increased complex viscosity. We believe this inflection was due to Col F elements spreading within the hydrogel that, upon dispersal, began to add to the viscoelastic properties of the system [14,15].

Collagen elements of the human hypodermis have a net positive charge that could favorably interact with net negatively charged HA or HA-XR. We also tested a hydrogel format where a negatively charged element of the human hypodermis was included. Chondroitin sulfate (CS), a sulfated glycosaminoglycan composed of alternating N-acetylgalactosamine and glucuronic acid residues, is one of the proteoglycans present in the human hypodermis which can have specific interactions with a variety of proteins [5]. CS incorporated into HA- or HA-XR-based hydrogels up to 0.3 mg/mL resulted in optically clear hydrogels at 4 °C that remained clear upon warming to 34 °C (Fig. 5**A, B**). Rheological analysis showed that HA- or HA-XR-based hydrogels containing 0.3 mg/mL CS showed comparable rheological properties to HA and HA-XR matrices alone (Fig. 5**C, D**). Compared to hydrogels where collagen proteins were introduced into HA or HA-XR, which resulted in a dose-dependent increase in optical density (Figs. 2-4), incorporation of net negatively charged, non-protein CS at 0.3 mg/mL into HA or HA-XR affected neither light transmission of these hydrogels nor their rheological properties.

3.2. *Impact of hydrogel components on solute diffusion properties*

3.2.1. *Dextran*

To appreciate how cross-linked HA and/or inclusion of other ECM

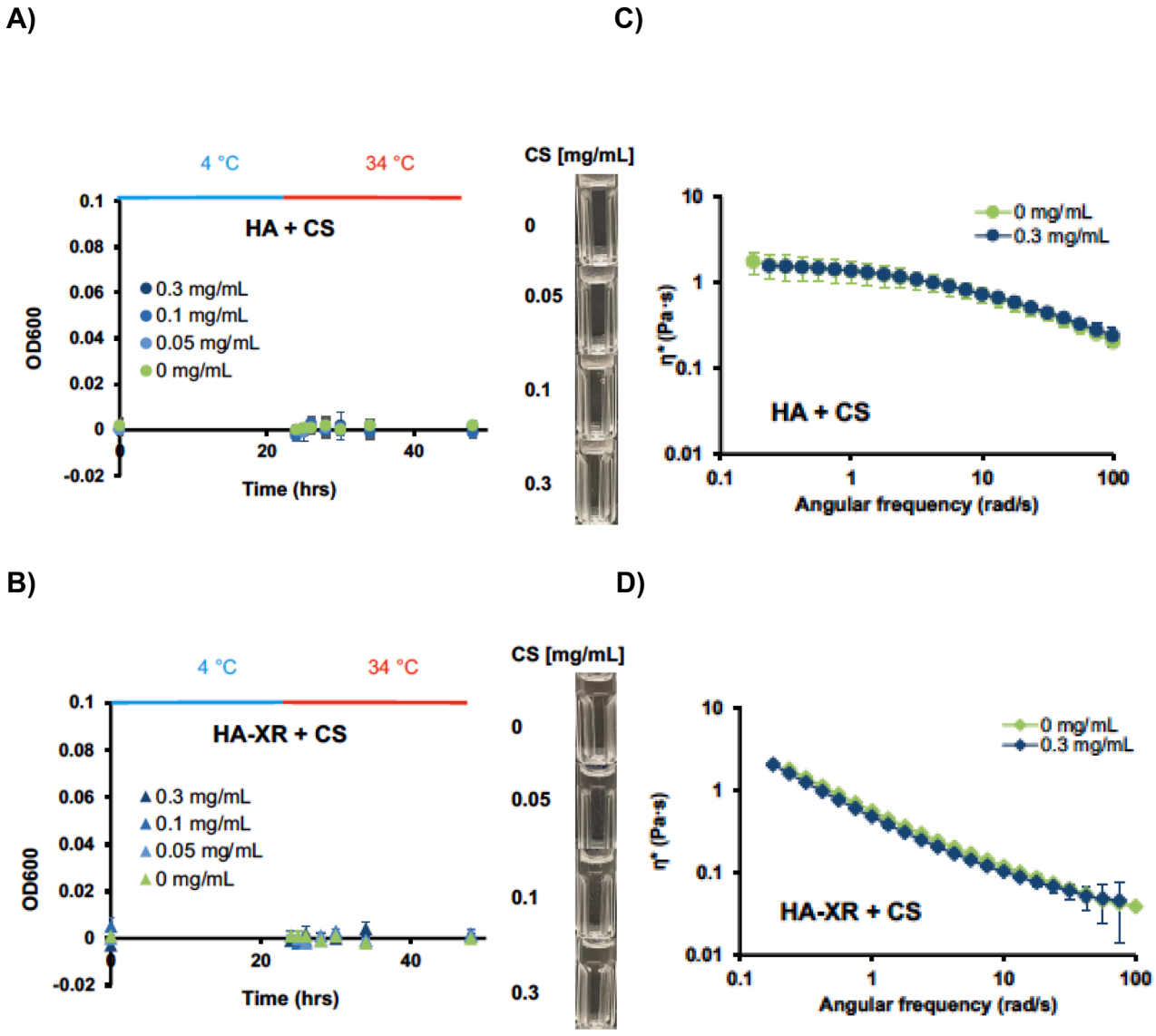

Fig. 5. Impact of chondroitin sulfate (CS) at 0.05, 0.1, or 0.3 mg/mL integrated into 6.25 mg/mL hyaluronic acid (HA) or 0.8 mg/mL cross-linked HA + 2.0 mg/mL HA (HA-XR) hydrogels. Assessment of optical clarity of (**A**) HA and (**B**) HA-XR hydrogels containing varying amounts of CS, where OD_{600} data represents n = 3 ± SEM with example cuvettes to enable a visual appreciation of relative opacity. (**C**) Angular frequency scans defining rheological properties of HA and HA-XR hydrogels with and without 0.3 mg/mL added CS. Complex viscosity (η*, Pa·s ± SD), shown as a function of angular frequency, was measured from 0.2-100 rad/s at 1 % strain in HA and HA-XR formats.

elements could affect API distribution, we first examined the distribution of fluorescently labeled, non-charged dextran, comparing materials with average molecular weight of 4 kDa (FD4) or 70 kDa (FD70). Release rates of FD4 or FD70 from cartridges containing 6.25 mg/mL HA were comparable over the first few hours with both demonstrating plateaus between 70–80 % release based upon mass balance (Fig. 6**A**). To explain the incomplete mass balance outcome, it is possible that HA leaving the cartridge during these studies could have masked (quenched) the fluorescence of these molecules during the latter stages of the experiment through HA-dextran interactions [16]. In support of this possibility were outcomes from studies where FD4 or FD70 were injected into aECM systems of 6.25 mg/mL HA + 0.05 mg/mL Col F; this demonstrated a size-dependent outcome for release of both FD4 or FD70 that ultimately reached 100 % recovery and with reduced variability compared to release profiles for HA alone (Fig. 6**A**).

As there were notable differences in FD70, but not FD4, release following injection into HA versus HA + Col F (Fig. 6**A**), we examined the physical distribution of FD70 following its injection into the SCISSOR cartridge. Here, we noted a more rapid distribution within the HA compared to HA + Col F (Fig. 6**B**), consistent with the release rates observed (Fig. 6**A**). Visual images showed that an initial elliptical-shaped bolus formed prior to diffusion throughout the top 1/3 of the cartridge. Injection into HA showed that this bolus diffused down through the cartridge while diffusing horizontally. FD70 injected into HA + Col F resulted in a more homogenous diffusion following initial bolus formation.

Visualization of materials injected into the hypodermis *in vivo* have shown that rather than a bolus, injected materials distribute through channel-like paths within the ECM that would be consistent with paths within a stabilized matrix that does not contain potential spaces for a bolus to form [17,18]. In this context, we examined the release of FD70 following its injection HA-XR and compared this to outcomes obtained following injection into HA-XR + Col F (Fig. 6**A**). For this study, we were particularly interested in examining the distribution of FD70 and the lower Col F level minimized potential optical density issues. A much slower release profile was observed compared to HA or HA + Col F,

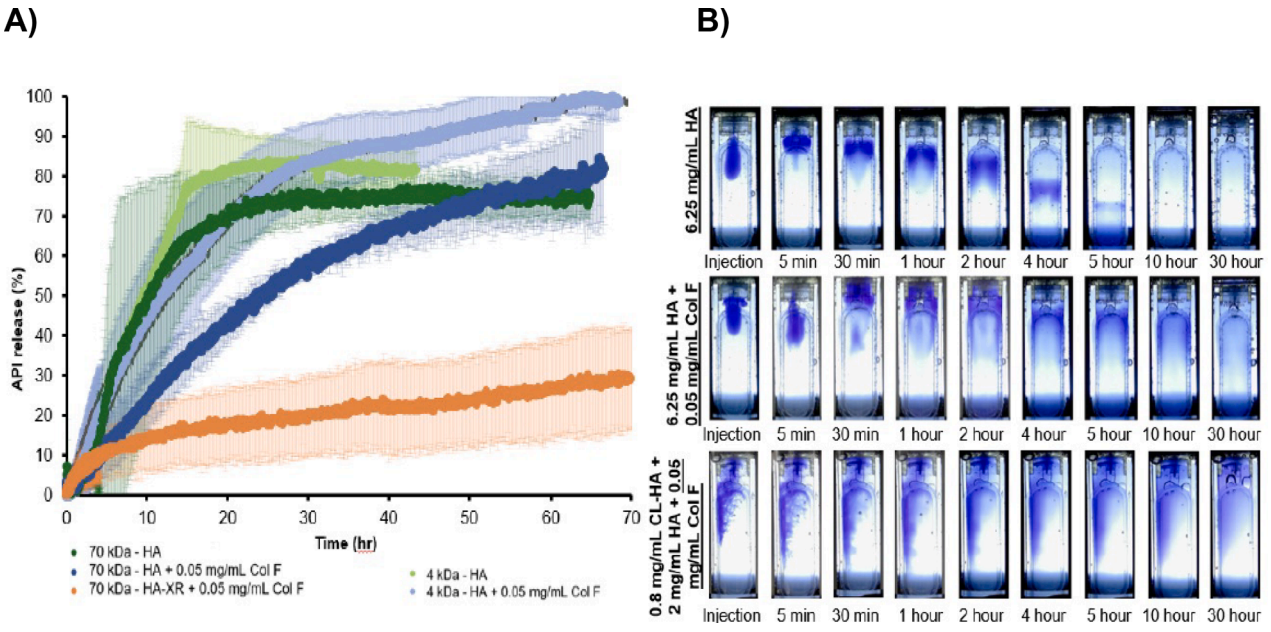

Fig. 6. Release profiles from and distribution within 6.25 mg/mL hyaluronic acid (HA) or 6.25 mg/mL HA plus 0.05 mg/mL collagen isolated from human fibroblasts (HA + Col F) of fluorescent dextran of 4 kDa (FD4) or 70 kDa (FD70) molecular weight. Additionally, release of FD70 from 6.25 mg/mL HA or 0.8 mg/mL crosslinked HA + 2.0 mg/mL HA (HA-XR) hydrogels containing 0.05 mg/mL Col F is shown. (**A**) The percentage of dose over time detected in interstitial fluid media to mimic the infinite sink of the body following 200 μL injections (n = 3, error bars = standard deviation). (**B**) Visualization of FD70 distribution over time following injection into 6.25 mg/mL HA, 6.25 mg/mL HA plus 0.05 mg/mL Col F, and 2.0 mg/mL HA + 0.8 mg/mL crosslinked HA (HA-XR) + 0.05 mg/mL Col F at the time of injection and at 0.083, 0.5, 1, 2, 4, 5, 10, and 30 h afterward.

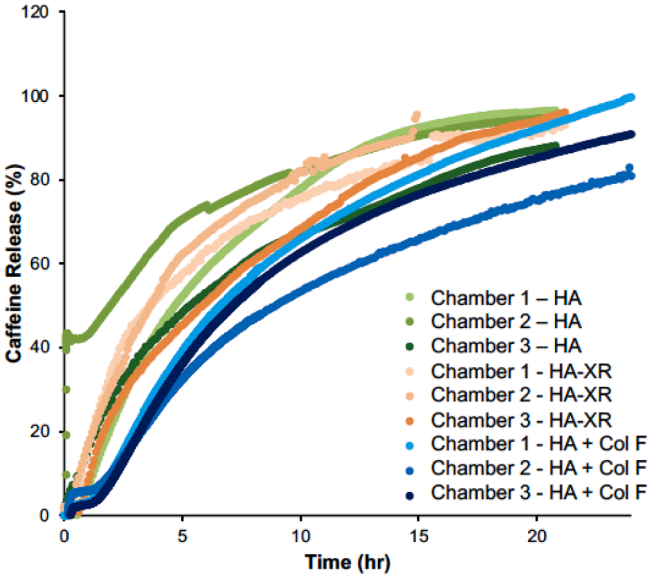

Fig. 7. Comparison of three independent release profiles of caffeine from hydrogels composed of 6.25 mg/mL hyaluronic acid (HA), 0.8 mg/mL crosslinked HA with 2.0 mg/mL HA (HA-XR), or 6.25 mg/mL HA + 0.01 mg/mL Col F. Real-time release of caffeine (200 μL injection of 10 mg/mL dissolved in PBS) was followed in the SCISSOR using the Rainbow spectrophotometer unit (Pion Inc., USA).

presumably due to a more elaborate and stable hydrogel matrix network. Consistent with this hypothesis, there was minimal bolus formation of FD70 injected into the SCISSOR cartridge containing HA-XR + Col F, with the injectate being initially spread through a greater volume of the cartridge.

3.3. Caffeine

Release of FD4 and FD70 from HA + Col F hydrogels showed less variability compared to the HA format (assessed by examining profiles of averages and standard errors for N = 3; Fig. 6**A**), suggesting that introduction of Col F could provide more consistent release rate outcomes than hydrogels composed of HA alone. To examine this more closely, we compared individual release rate profiles of the small molecule drug caffeine following injection into SCISSOR cartridges containing a 6.25 mg/mL HA versus 6.25 mg/mL HA + 0.1 mg/mL Col F and compared these outcomes to that obtained following injection into a 0.8 mg/mL CL-HA with 2.0 mg/mL HA (HA-XR) hydrogel matrix (Fig. 7). Caffeine, a water-soluble molecule with a mass of 194 g/mol and a net positive charge at neutral pH, was released rapidly from SCISSOR cartridges containing either HA or HA-XR formats into the receiver (ISF) media, with one cartridge demonstrating substantial caffeine release at the first measurement points. This instantaneous release was not observed for injections made into HA-XR or HA + Col F, possibly due to increased hydrogel organization. It was also noted that while all three hydrogel formats showed complete caffeine release, there was a consistent initial lag of caffeine release from the HA + Col F hydrogel compared to HA and HA-XR matrices, suggesting that this aECM element also slowed initial caffeine diffusion in the hydrogel. Following this initial lag observed for HA + Col F hydrogels, release rates for all three formats for this small molecule appeared comparable. Comparison between separate hydrogel systems would require similar behavior of injectates that don't have a specific interaction with the included ECM components.

3.4. Insulin

We compared release rates of two insulin formulations designed for prandial (Actrapid®) or basal (Levemir®) control of blood sugar. The rapid or slower rate of insulin reaching the systemic circulation following SC injection site is due to protein solubility and protein–protein interactions of these two medicines [19]. Release of prandial insulin

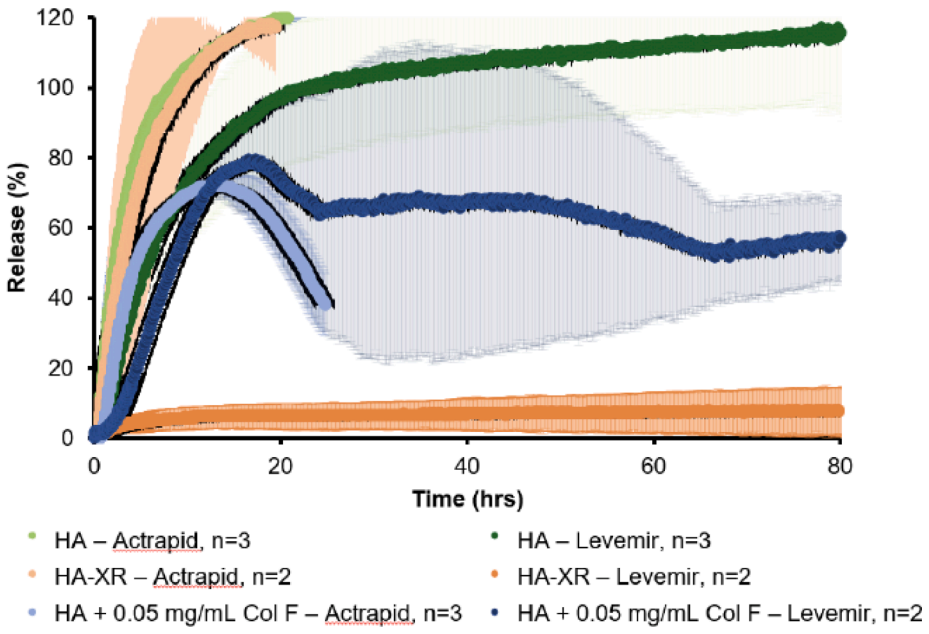

Fig. 8. Release profiles of prandial (Actrapid®) or basal (Levemir®) insulins following injection of 50 μL volumes into SCISSOR cartridges containing hydrogels of 6.25 mg/mL hyaluronic acid (HA), 2.0 mg/mL HA + 0.8 mg/mL cross-linked HA (HA-XR), or 6.25 mg/mL HA + 0.05 mg/mL Col F. Insulin was detected in the ISF receptor chamber in situ via a Rainbow spectrophotometry unit (Pion, Inc., USA). Error bars = standard deviation. N = 3 for HA Prandial, HA Basal, and HA + Col F Prandial. N = 2 for HA-XR Prandial, HA-XR Basal, and HA + Col F Basal.

from the hydrogel of 6.25 mg/mL HA following injection was rapid, with basal insulin showing a delayed release by comparison (Fig. 8). The overall release of insulin into the ISF receiver compartment was calculated to reach 120 %, which was likely an issue of spectrophotometric measurement of insulin resulting from its dynamic and complex self-association properties [20]. Inclusion of 0.05 mg/mL Col F into the HA hydrogel slowed insulin release, with our method of detection suggesting only ~ 70 % of prandial insulin being released by 10 h and ~ 80 % of basal insulin being released by 15 h. We again observed an improbable mass loss of prandial insulin after 10 h and extensive variability of basal insulin within a similar timescale in the ISF suggesting complications with our spectroscopic detection method of these materials, possibly due to their dynamic and complex self-association properties [20]. Release of prandial insulin from the HA-XR hydrogel matrix followed similar kinetics to that observed for HA, while less than 10 % of basal insulin injected into HA-XR was released after 80 h (Fig. 8). These differences observed between prandial and basal insulins in the HA-XR format appear to reflect how variations in formulations may be augmented in certain hydrogel formats.

3.5. Denosumab

We next compared the impact of different levels of Col F on the release properties of denosumab (Prolia®), a monoclonal antibody administered by SC injection once every six months to treat osteoporosis [21]. Monoclonal antibodies can exhibit self-associating behavior that can be affected by environmental conditions, possibly affecting their release from a SC injection site [22]. Prolia® was injected into SCISSOR cartridges containing a hydrogel composed of 6.25 mg/mL HA or HA containing 0.05 mg/mL or 0.1 mg/mL Col F. Complete release of denosumab from HA occurred within 72 hrs; the cause of a mass balance recovery of > 100 % in these studies is unclear. By comparison, the extent of denosumab released from SCISSOR cartridges containing 6.25 mg/mL HA + 0.05 or 0.1 mg/mL Col F resulted in initial release rates comparable to that observed for cartridges containing HA alone. These rate, however, differed later with HA + 0.05 mg/mL Col F hydrogel plateauing at ~ 70 % released while release from the HA + 0.1 mg/mL Col F hydrogel reached a slightly lower plateau of ~ 65 % released (Fig. 9**A**). Release of denosumab from cartridges containing HA-XR showed slower rates than the HA + Col F hydrogel formats but with a comparable release plateau outcome. These release profiles were consistent with either Col F in the HA or cross-linked HA present in the HA-XR resulting in more stable hydrogel formats useful for examining API release over multiple days (Fig. 1).

Visual examination of a SCISSOR cartridge containing a HA + 0.1 mg/mL Col F hydrogel from one experiment showed dispersed the injected material to be flocculated, presumably reflecting a change in denosumab solubility that became noticeable by 3 hrs post injection (Fig. 9**B**). This increase in optical turbidity increased by 30 hrs after injection. The plateau in antibody release from the SCISSOR cartridge correlated with the onset of an increase in optical turbidity, that reached a maximum by 62 hrs and remained visible for the remainder of the study. A time profile of pH measured within the cartridge and optical density of the hydrogel following Prolia® injection demonstrated that changes in pH inversely correlated with flocculation (Fig. 9**C**). Such changes in denosumab solubility at the injection site would be consistent with the long-acting behavior of this antibody formulation in patients [23].

3.6. Bevacizumab

Finally, we explored the HA versus HA + Col F hydrogel systems to model how an ECM element could affect the release of a therapeutic agent from the SC injection site. A variety of growth factor proteins can bind tightly to ECM elements, including collagen, providing a mechanism where their activity is regulated through release via restricted proteolysis [24]. In its native form of 206 amino acids, vascular endothelial growth factor (VEGF) is a heparin-binding homodimeric glycoprotein of 45 kDa, with the properties of native VEGF closely corresponding to a shortened version of $VEGF_{165}$ that was obtained from Genentech, Inc. While $VEGF_{165}$ is almost completely sequestered in the ECM, the proteolytic $VEGF_{121}$ fragment is an acidic polypeptide that can freely diffuse through the ECM [25]. The monoclonal antibody bevacizumab (Avastin®) targets the receptor-active region of $VEGF_{121}$ to impede tumor growth by suppressing neovascularization [26].

Avastin® (200 μL) injected into 6.25 mg/mL HA demonstrated a

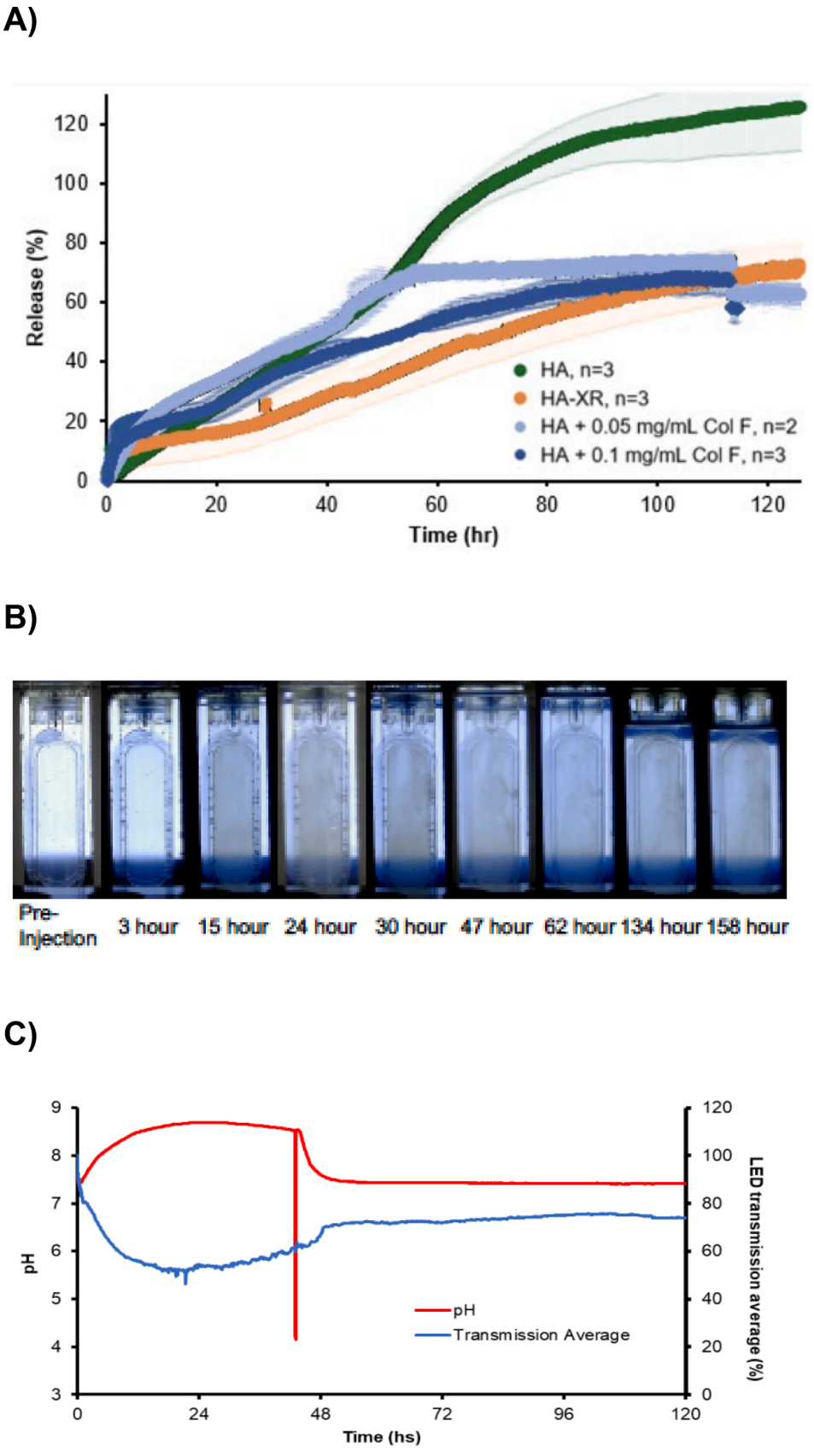

Fig. 9. (**A**) Time course of denosumab release following a 200 μL injection of Prolia® into SCISSOR cartridges containing 6.25 mg/mL hyaluronic acid (HA), HA + 0.05 or 0.1 mg/mL of collagens isolated from human fibroblasts (HA + Col F), or 0.8 mg/mL cross-linked HA + 2.0 mg/mL HA (HA-XR). HA (n = 3), HA + 0.1 mg/mL Col F (n = 3), HA-XR (n = 3), HA + 0.05 mg/mL Col F (n = 2). (**B**) Visual examination of HA + 0.1 mg/mL Col F of cartridge from one experiment over time following 200 μL injection of Prolia®. (**C**) Time profile of optical density (averaged from the four diode detectors of the SCISSOR) and pH measured within the hydrogel following a 200 μL injection of Prolia® into HA + 0.1 mg/mL Col F of cartridge.

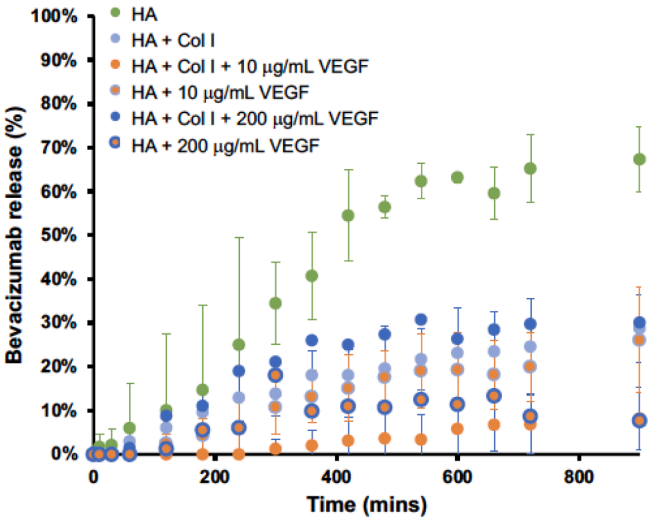

Fig. 10. Time course of bevacizumab release following a 200 µL injection of (Avastin®) into SCISSOR cartridges containing either 6.25 mg/mL hyaluronic acid (HA) or HA + 0.05 mg/mL bovine type 1 collagen (Col I). Some hydrogels also contained 10 or 200 µg/mL $VEGF_{165}$. N = 3 for all tests except HA + 200 µg/mL VEGF (N = 2).

bevacizumab release curve that plateaued after 6–7 hrs (Fig. 10), similar to previous SCISSOR studies on this class of antibody [6,7]. Introduction of 10 µg/mL $VEGF_{165}$ into the HA hydrogel delayed release of bevacizumab (Fig. 10), consistent with the formation of bevacizumab-$VEGF_{165}$ complexes that were retained by interactions with HA. Avastin® injection into HA + 0.05 mg/mL Col I demonstrated only limited release of bevacizumab from the SCISSOR cartridge, being minimally affected by the presence of $VEGF_{165}$ (Fig. 10). Together, these studies suggest extensive interactions between bevacizumab and Col F as well as the potential for additional interactions involving its therapeutic target that also has ECM binding properties. Such studies demonstrated that the SCISSOR instrument could be used to model complex events that might occur following SC administration where an injected API could interact not only with ECM elements, but also with non-ECM elements retained in the hypodermis through separate sets of interactions.

4. Discussion

The human hypodermis is a complex hydrogel composed of multiple protein and polysaccharide-based materials that is frequently used for the administration of various classes of biopharmaceuticals; its unique properties among the animal kingdom is exemplified by the fact that no other species provides broadly comparable bioavailability outcomes for SC injected medicines [3]. This lack of a predictive preclinical model has important consequences for the pharmaceutical companies attempting to identify a lead candidate, preferred formulation, or rationalize clinical anomalies for a biopharmaceutical agent intended for SC injection [27]. While it is unrealistic to establish a readily accessible *in vitro* tool that models all complexities of the human hypodermis [28], it is possible to examine specific aspects of possible events that could occur through interaction(s) between a biopharmaceutical and ECM elements. Indeed, agarose hydrogels have been used to mimic certain properties of the SC injection site to predict parenteral drug formulation performance [29]. We established the SCISSOR instrument as an *in vitro* using an HA hydrogel to model drug fate following SC injection, information that can be used examine drug and formulation risks [30]. In the present studies, we have described a set of hydrogels containing some highly represented components of the hypodermis to determine if such matrices could be used in the SCISSOR instrument to expand the experimental options of this tractable model. Critically, we worked toward the identification of aECM formats where sufficient optical clarity was retained to allow visual examination assessment of potential drug solubility issues. We also sought to maintain comparable rheological properties following addition of an ECM element to allow direct comparisons of drug release observed between these different hydrogels. For HA, the addition of ECM elements failed to affect frequency scan profiles beyond the standard error of the system. Collagen additions to the HA-XR format, however, did add significantly to the viscosity of these systems.

It is not possible to make in-depth interpretations from the limited set of studies described. The focus of these studies was to validate a repertoire of hydrogel matrices as tools that can now be used by pharmaceutical scientists to perform more extensive studies where hypothesis-driven questions regarding specific interactions between drug molecules and ECM elements of the hypodermis as well as the impact of formulation components could be examined. Further, we did not attempt to examine the vast number of possible combinations and permutations for each of these molecules with the various hydrogel systems described. Therefore, our data was intended to encompass representative systems intended only for validation of the analysis potential of similar hydrogel-based systems. While the idea that drug delivery systems with reduced drug interactions with tissues would be a focus of the pharmaceutical industry, this set of aECM formats could be used to work toward this goal for assessing subcutaneous formulations.

Hydrogels tested in the current studies were not intended to completely replicate the human hypodermis architecture within the SCISSOR cartridge. Instead, our aim was to extend the repertoire of injection site formats available for SCISSOR-based studies and to examine the impact of individual ECM elements present in the human hypodermis on the fate of injected molecules. This is a tractable system, designed to probe the effects of a specific element in the system. For such studies, absolute levels of these elements are not as important as their presence and we show that collagen from human fibroblasts (Col F), bovine type I collagen (Col I), chicken collagen type II (Col II), or chondroitin sulphate (CS) can be integrated into HA hydrogels to produce systems amenable for this use. Of the ECM elements examined, we did not identify a clinically relevant question to assess. As proteoglycan-(PG) forming glycosaminoglycans and chondroitin sulfate PGs present in the human hypodermis can facilitate collagen fibril formation [31] these hydrogel matrices may find applications in formulation strategies to alter interactions with collagens [32]. While we focused on introduction of these components individually, each could be incorporated in combinations with other ECM elements to explore the impact of their combined integration into these hydrogels. Our studies showed that Col F containing predominantly human type I collagen and bovine Col I had similar properties in these hydrogels and produced similar experimental outcomes, making Col F the preferred material for future work examining the impact of human collagen. While there is potential for including other ECM elements, availability and/or practicality of incorporating these materials into a hydrogel within a SCISSOR cartridge will need to be considered.

One of the issues addressed in these studies is the loss of HA within the SCISSOR cartridge overt extended (multiple days) periods of time. While HA alone can provide a hydrogel format to assess release properties over a few hours, its loss from the SCISSOR cartridge was slowed by the inclusion of collagens where non-covalent complexation could be occurring or the introduction of chemical cross-linking of HA molecules themselves. The current studies have described and characterized several HA-based hydrogel formats amenable for measuring extended-release profiles required to assess LAI formulations and potential interactions with specific ECM elements that might affect the performance of a SC injected formulation. While these hydrogel formats have focused on optical clarity and manageable viscosities, we are not suggesting that these exactly replicate properties of the human hypodermis. Indeed, is it unlikely that the ECM of the human hypodermis is optically clear or could be readily transferred into a SCISSOR cartridge. Hydrogel formats described in these studies are intended to extend the repertoire of experimental formats that can be used to address hypothesis-driven

questions to accelerate the rational identification and initial *in vitro* testing of formulations intended for SC administration.

CRediT authorship contribution statement

Conor Gomes: Writing – original draft, Investigation, Formal analysis, Data curation, Conceptualization. **Kate Gridley:** Writing – original draft, Methodology, Investigation, Formal analysis, Data curation. **Imogen Anastasiou:** Validation, Resources, Formal analysis. **Bálint Sinkó:** Visualization, Supervision, Methodology, Investigation, Funding acquisition, Conceptualization. **Randall J. Mrsny:** Writing – review & editing, Writing – original draft, Supervision, Methodology, Funding acquisition, Conceptualization.

Declaration of competing interest

The authors declare that they have no known competing financial interests or personal relationships that could have appeared to influence the work reported in this paper.

Data availability

Data will be made available on request.

Acknowledgements

Randy Mrsny thanks the Wellcome Trust for being a Value in People recipient. This work was funded by Pion Inc.

References

[1] D.S. Collins, L.C. Kourtis, N.R. Thyagarajapuram, R. Sirkar, S. Kapur, M. W. Harrison, D.J. Bryan, G.B. Jones, J.M. Wright, Optimizing the bioavailability of subcutaneously administered biotherapeutics through mechanochemical drivers, Pharm. Res. 34 (2017) 2000–2011.
[2] I. Torres-Teran, M. Venczel, T. Stieler, L. Parisi, A. Kloss, S. Klein, Prediction of subcutaneous drug absorption - characterization of subcutaneous interstitial fluids as a basis for developing biorelevant in vitro models, Int. J. Pharm. 122906 (2023).
[3] H.M. Kinnunen, R.J. Mrsny, Improving the outcomes of biopharmaceutical delivery via the subcutaneous route by understanding the chemical, physical and physiological properties of the subcutaneous injection site, J. Control. Release 182 (2014) 22–32.
[4] N. Nishi, O. Matsushita, K. Yuube, H. Miyanaka, A. Okabe, F. Wada, Collagen-binding growth factors: production and characterization of functional fusion proteins having a collagen-binding domain, Proc. Natl. Acad. Sci. USA 95 (1998) 7018–7023.
[5] L. Djerbal, H. Lortat-Jacob, J. Kwok, Chondroitin sulfates and their binding molecules in the central nervous system, Glycoconj. J. 34 (2017) 363–376.
[6] H.M. Kinnunen, V. Sharma, L.R. Contreras-Rojas, Y. Yu, C. Alleman, A. Sreedhara, S. Fischer, L. Khawli, S.T. Yohe, D. Bumbaca, T.W. Patapoff, A.L. Daugherty, R. J. Mrsny, A novel in vitro method to model the fate of subcutaneously administered biopharmaceuticals and associated formulation components, J Control Release 214 (2015) 94–102.
[7] H.K. Bown, C. Bonn, S. Yohe, D.B. Yadav, T.W. Patapoff, A. Daugherty, R.J. Mrsny, In vitro model for predicting bioavailability of subcutaneously injected monoclonal antibodies, J Control Release 273 (2018) 13–20.
[8] S. Kim, S. Min, Y.S. Choi, S.H. Jo, J.H. Jung, K. Han, J. Kim, S. An, Y.W. Ji, Y. G. Kim, S.W. Cho, Tissue extracellular matrix hydrogels as alternatives to Matrigel for culturing gastrointestinal organoids, Nat Commun 13 (2022) 1692.
[9] https://www.pion-inc.com/resources.
[10] A. Martinez-Ortega, A. Herrera, A. Salmeron-Garcia, J. Cabeza, L. Cuadros-Rodriguez, N. Navas, Validated reverse phase HPLC diode array method for the quantification of intact bevacizumab, infliximab and trastuzumab for long-term stability study, Int J Biol Macromol 116 (2018) 993–1003.
[11] C.L. Martin, M.R. Bergman, L.F. Deravi, J.A. Paten, A Role for Monosaccharides in Nucleation Inhibition and Transport of Collagen, Bioelectricity 2 (2020) 186–197.
[12] D. Mishra, S. Gade, K. Glover, R. Sheshala, T.R.R. Singh, Vitreous Humor: Composition, Characteristics and Implication on Intravitreal Drug Delivery, Curr Eye Res 48 (2023) 208–218.
[13] R. Naomi, P.M. Ridzuan, H. Bahari, Current Insights into Collagen Type I, Polymers (basel) 13 (2021).
[14] L.A. Shah, T.U. Rehman, M. Khan, Synthesis of graphene oxide doped poly(2-acrylamido-2-methyl propane sulfonic acid) [GO@p(AMPS)] composite hydrogel with pseudo-plastic thixotropic behavior, Polym Bull 77 (2020) 3921–3935.
[15] X.N. Ye, T. Sridhar, Effects of the polydispersity on rheological properties of entangled polystyrene solutions, Macromolecules 38 (2005) 3442–3449.
[16] Y. Luo, J.B. Kobler, J.T. Heaton, X. Jia, S.M. Zeitels, R. Langer, Injectable hyaluronic acid-dextran hydrogels and effects of implantation in ferret vocal fold, J Biomed Mater Res B Appl Biomater 93 (2010) 386–393.
[17] M. Thomsen, M. Poulsen, M. Bech, A. Velroyen, J. Herzen, F. Beckmann, R. Feidenhans'l, F. Pfeiffer, Visualization of subcutaneous insulin injections by x-ray computed tomography, Phys Med Biol 57 (2012) 7191–7203.
[18] M. Thomsen, C.H. Rasmussen, H.H. Refsgaard, K.M. Pedersen, R.K. Kirk, M. Poulsen, R. Feidenhans'l, Spatial distribution of soluble insulin in pig subcutaneous tissue: Effect of needle length, injection speed and injected volume, Eur J Pharm Sci 79 (2015) 96–101.
[19] A.K.J. Gradel, T. Porsgaard, J. Lykkesfeldt, T. Seested, S. Gram-Nielsen, N. R. Kristensen, H.H.F. Refsgaard, Factors Affecting the Absorption of Subcutaneously Administered Insulin: Effect on Variability, J Diabetes Res 2018 (2018) 1205121.
[20] J. Brange, L. Andersen, E.D. Laursen, G. Meyn, E. Rasmussen, Toward understanding insulin fibrillation, J Pharm Sci 86 (1997) 517–525.
[21] D.L. Kendler, F. Cosman, R.K. Stad, S. Ferrari, Denosumab in the Treatment of Osteoporosis: 10 Years Later: A Narrative Review, Adv Ther 39 (2022) 58–74.
[22] W.G. Lilyestrom, S. Yadav, S.J. Shire, T.M. Scherer, Monoclonal antibody self-association, cluster formation, and rheology at high concentrations, J Phys Chem B 117 (2013) 6373–6384.
[23] H. Chen, W. Chen, F. Yuan, Q. Guo, X. Zhang, C. Wang, X. Li, Pharmacokinetics, Pharmacodynamics, Safety and Immunogenicity of CMAB807, a New Denosumab Biosimilar, in Healthy Chinese Subjects, Front Pharmacol 13 (2022) 821944.
[24] M.M. Martino, P.S. Briquez, A. Ranga, M.P. Lutolf, J.A. Hubbell, Heparin-binding domain of fibrin(ogen) binds growth factors and promotes tissue repair when incorporated within a synthetic matrix, Proc Natl Acad Sci U S A 110 (2013) 4563–4568.
[25] N. Ferrara, H.P. Gerber, J. LeCouter, The biology of VEGF and its receptors, Nat. Med. 9 (2003) 669–676.
[26] K. Haraya, T. Tachibana, Estimation of clearance and bioavailability of therapeutic monoclonal antibodies from only subcutaneous injection data in humans based on comprehensive analysis of clinical data, Clin. Pharmacokinet. 60 (2021) 1325–1334.
[27] M. Sanchez-Felix, M. Burke, H.H. Chen, C. Patterson, S. Mittal, Predicting bioavailability of monoclonal antibodies after subcutaneous administration: Open innovation challenge, Adv. Drug Deliv. Rev. 167 (2020) 66–77.
[28] L. Weber, E. Kirsch, P. Muller, T. Krieg, Collagen type distribution and macromolecular organization of connective tissue in different layers of human skin, J. Invest. Dermatol. 82 (1984) 156–160.
[29] D.H. Leung, Y. Kapoor, C. Alleyne, E. Walsh, A. Leithead, B. Habulihaz, G. M. Salituro, A. Bak, T. Rhodes, Development of a convenient in vitro gel diffusion model for predicting the in vivo performance of subcutaneous parenteral formulations of large and small molecules, AAPS PharmSciTech 18 (2017) 2203–2213.
[30] S. Thati, M. McCallum, Y. Xu, M. Zheng, Z. Chen, J. Dai, D. Pan, D. Dalpathado, N. Mathias, Novel applications of an in vitro injection model system to study bioperformance: case studies with different drug modalities, J. Pharm. Innov. 15 (2020) 268–280.
[31] D. Chen, L.R. Smith, G. Khandekar, P. Patel, C.K. Yu, K. Zhang, C.S. Chen, L. Han, R.G. Wells, Distinct effects of different matrix proteoglycans on collagen fibrillogenesis and cell-mediated collagen reorganization, Sci. Rep. 10 (2020) 19065.
[32] A.M. Curreri, J. Kim, M. Dunne, P. Angsantikul, M. Goetz, Y. Gao, S. Mitragotri, Deep eutectic solvents for subcutaneous delivery of protein therapeutics, Adv. Sci. (weinh.) 10 (2023) e2205389.